

Large photoconductivity of oxygen-deficient $\text{La}_{0.7}\text{Ca}_{0.3}\text{MnO}_3/\text{SrTiO}_3$ heterostructures

This article has been downloaded from IOPscience. Please scroll down to see the full text article.

2010 J. Phys.: Condens. Matter 22 175506

(<http://iopscience.iop.org/0953-8984/22/17/175506>)

View [the table of contents for this issue](#), or go to the [journal homepage](#) for more

Download details:

IP Address: 129.252.86.83

The article was downloaded on 30/05/2010 at 07:55

Please note that [terms and conditions apply](#).

Large photoconductivity of oxygen-deficient $\text{La}_{0.7}\text{Ca}_{0.3}\text{MnO}_3/\text{SrTiO}_3$ heterostructures

E Beyreuther¹, A Thiessen¹, S Grafström¹, K Dörr² and L M Eng¹

¹ Institute of Applied Photophysics, Technische Universität Dresden, D-01062 Dresden, Germany

² Institute for Metallic Materials, IFW Dresden, D-01171 Dresden, Germany

E-mail: elke.beyreuther@iapp.de

Received 29 January 2010, in final form 12 March 2010

Published 12 April 2010

Online at stacks.iop.org/JPhysCM/22/175506

Abstract

The electrical resistance of stoichiometric and oxygen-deficient epitaxial 10 nm thick $\text{La}_{0.7}\text{Ca}_{0.3}\text{MnO}_3$ thin films on SrTiO_3 under photoexcitation covering the visible to the ultraviolet range has been investigated systematically as a function of illumination intensity, wavelength and temperature. In contrast to as-prepared films, the oxygen-deficient samples exhibit large photoconductivity of several orders of magnitude at low temperatures. By our detailed comparative analysis of the electrical conductivity of the film/substrate heterostructure and the bare substrate we are able to elucidate contributions of both carrier generation in the film and carrier injection from the substrate to the observed effect.

1. Introduction

Perovskite-type manganites $(\text{R}, \text{A})\text{MnO}_3$ (R = lanthanide-element, A = non-trivalent doping element) are well known to exhibit an unusually broad spectrum of electronic, magnetic and optical properties, which makes them promising candidates for novel solutions in micro- or optoelectronics.

The actual phase state of those compounds can be controlled by internal parameters, especially the concentration of the doping element A and the oxygen content, and a number of external parameters such as static magnetic and electric fields, hydrostatic pressure and photoexcitation [1–3]. The fact that nowadays high-quality epitaxial thin films can be grown on structurally compatible perovskite-type substrates further enlarges the variety of tunable functional properties.

With regard to more than 50 years of research on manganites, the investigation of photoinduced phenomena is quite a new field. It started in 1997, when Kiryukhin *et al* found an x-ray-induced insulator–metal transition combined with a clear structural change in a $\text{Pr}_{0.7}\text{Ca}_{0.3}\text{MnO}_3$ single crystal [4]. In the meantime a number of studies on the photoexcitation of manganites from the x-ray to the infrared wavelength range have been published, see, for example, [5–13]. In most cases positive photoconductivity has been observed, which can, comparable to the colossal magnetoresistance (CMR) effect, reach several orders of magnitude.

In some manganite compounds a reversible photoinduced transition from an insulating to a metastable metal phase was reported [14]. In this context the term *optical phase control* was established [15].

The transient behaviour of photoconduction is often substantially influenced by the electrical field or current applied for the conduction measurement [13, 16–19].

The conductive state is not spatially homogeneous in a number of photoconductive manganites but filament-like conduction paths in an insulating matrix are generated (e.g. [16]).

By now, there is no general understanding of the involved microscopic mechanisms available. Several origins of the photoconduction in manganites have been discussed. First of all, it is argued that photoexcitation above the polaron binding energy leads to the delocalization of charge carriers. The polaron binding energy results from the strong Jahn–Teller effect of the Mn^{3+} ions and a possible long-range polaron order. In some insulating manganites an ordered lattice of singly occupied 3d e_g orbitals is present which can—under sufficiently strong optical excitation—undergo a collective charge delocalization and a transition into a metastable metal phase. Secondly, the influence of the measurement current has been discussed qualitatively: since the carrier transport is spin-polarized requiring the alignment of the carrier spins with the local magnetic moment of the Mn ions, a forced current

will act to align the Mn spins along the current path [20]. Thus the current can stabilize the metallic phase at least in the filaments of the conduction path. Further mechanisms discussed are optically induced local heating [21], a magnetic depolarization under illumination [22] and the trapping of photogenerated carriers at oxygen vacancies [7]. Recently, the resonant excitation of electrons from deep Mn 3p levels in an ultraviolet photoemission experiment was discussed as another possible origin of photoconductivity in a manganite [23].

Although many photoexcitation experiments were performed with films, the contribution of a potential charge injection from the substrate or the film/substrate interface so far has been rarely considered. One exception is the investigation of Katsu *et al* conducted on $\text{La}_{1-x}\text{Sr}_x\text{MnO}_3/\text{SrTiO}_3$ films [24], where the authors demonstrate by a systematic study of resistance and magnetization under illumination that electrons from the substrate are injected into the manganite film, which leads to a decrease of the hole doping in the film. In recent work on an electron-doped manganite film we show a substantial substrate contribution in the spectral dependence of the photoconductivity [25]. Both examples clearly show the necessity to examine not only the film but also the substrate and the film/substrate interface in such photoconduction experiments, when the films are thinner than the absorption length of light (in the range of several 10 nm depending on the material of the film).

The present study focuses on the photoresponse behaviour of ultra-thin (10 nm) films of $\text{La}_{0.7}\text{Ca}_{0.3}\text{MnO}_3$ on SrTiO_3 . The photoconductivity of the films in the as-prepared hole-doped state is compared to that of oxygen-reduced films. The latter have an electron-doped nature according to our former photoelectron spectroscopy results [26]. To clarify possible origins of the photoconductivity the transport behaviour of bare SrTiO_3 substrates is also studied.

2. Experimental details

10 nm thick films of $\text{La}_{0.7}\text{Ca}_{0.3}\text{MnO}_3$ (LCMO) were grown on an $\text{SrTiO}_3(100)$ single-crystal substrate by pulsed-laser deposition in off-axis geometry [27]. A stoichiometric target was ablated with a KrF excimer laser at a wavelength of 248 nm. X-ray diffraction measurements were employed to ensure single-phase epitaxial growth.

The samples were cut into two halves of $10 \times 5 \times 0.5 \text{ mm}^3$ each. One half was deoxygenated by heating it for 2 h in an ultrahigh vacuum (UHV) at 670°C . Both halves, the deoxygenated and the as-prepared one, were analysed with regard to their manganese valence and thus to their doping type by x-ray photoelectron spectroscopy, as described in detail elsewhere [26]. The as-prepared film showed a Mn valence between +3 and +4 and is thus, as expected, hole-doped. The deoxygenated film turned out to be electron-doped with an Mn valence between +2 and +3.

For electrical transport measurements the samples were fixed on a sapphire slide sitting on the sample holder of an exchange-gas liquid-nitrogen optical cryostat (Optistat DN by Oxford Instruments). Metallic contacts were painted on the film surfaces by conductive silver paste. The resistance

was measured by a Keithley 617 electrometer in two-point geometry using coaxial wiring down to the sample. The distance between the contacts was 1 mm.

To check possible contributions of the SrTiO_3 (STO) substrate to the photoconductivity, transport measurements were additionally performed on reference substrates: on a substrate as purchased from the manufacturer and on one which had undergone the same vacuum annealing treatment as the deoxygenated manganite film.

For exploring the photoresponse of the specimens, the sample surfaces were illuminated by either an Ar^+ laser (Coherent Innova 90) operated in the cw mode at a wavelength of 514 nm or, especially to investigate the spectral behaviour of the photoresponse, by a monochromatized white-light source (1000 W xenon arc lamp coupled into a grating monochromator (Cornerstone 260 by Oriel Instruments)).

When measured in two-point geometry, the resistance value comprises also the contact resistance, which may skew the data. In order to estimate the contact resistance, we additionally made a four-point measurement on the as-prepared film. We found that the contact resistance is insignificant at room temperature, but can reach up to approximately 1 M Ω at 100 K. In most cases this is still far below the measured total resistance and hence negligible. Where after all the contact resistance could distort the data, this will be noted in the corresponding figure caption (in fact this applies to only one single case, figure 1(b)). Note that, as the silver paste used for the contacts was opaque, we do not expect the contact resistance to change under illumination.

3. Results and discussion

The *as-prepared* $\text{La}_{0.7}\text{Ca}_{0.3}\text{MnO}_3/\text{SrTiO}_3$ sample exhibits an insulating R - T characteristic in the dark (figure 1(a), black curve). No insulator-metal transition is observed, in contrast to the bulk LCMO phase of the same composition. The insulating nature of the film is attributed to the combination of high tensile strain due to the larger lattice constant of the substrate and the finite thickness of the film, which are known to suppress the metallic phase [3, 28].

Under photoexcitation with energies below the substrate bandgap (3.2 eV, 387 nm) a small *increase* of the resistance (figure 1(a), grey curves) is observed. This effect is the more pronounced the lower the temperature is. Photons with energies around or above the substrate bandgap induce a local maximum in the R - T characteristics (figure 1(b)). The position of this maximum slightly shifts towards higher temperatures with larger excitation energy. However, the maximum resistance drop induced by photoexcitation found here (370 nm, near 100 K) is smaller than one order of magnitude.

Concerning possible origins of the photoinduced resistance changes the following points are considered:

- (i) The thickness of the film is much lower than the absorption length of light in the wavelength range used in the present experiments. Thus not only the film but also the substrate is optically excited. Consequently,

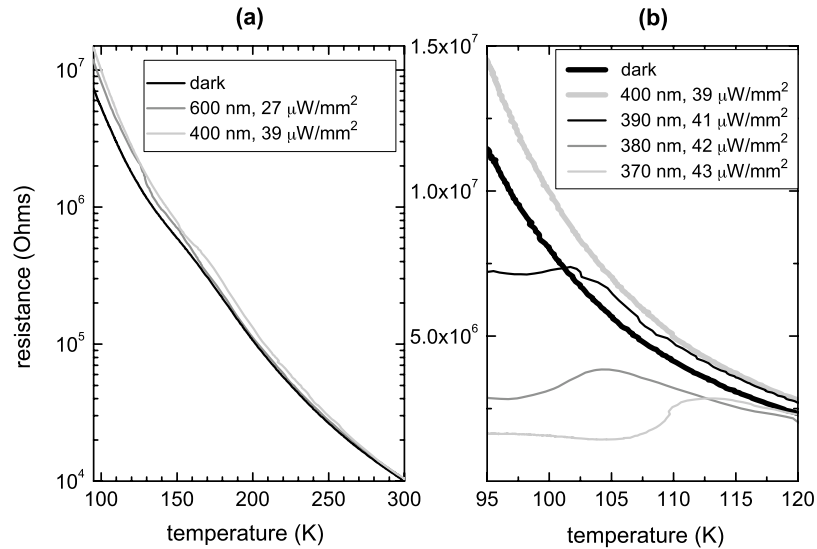


Figure 1. As-prepared $\text{La}_{0.7}\text{Ca}_{0.3}\text{MnO}_3$ film on SrTiO_3 : (a) resistance measured as a function of temperature in the dark and under illumination with two different photon energies *below* the substrate bandgap. (b) R - T -characteristics under photoexcitation with photon energies around and *above* the SrTiO_3 bandgap. Note the expanded temperature scale in this plot. Furthermore, note that for excitation at 370 nm the measured resistance drop at the lowest temperatures might be limited by the contact resistance.

all observed effects can—in principle—have their origin either in processes in the substrate or in the film, or in both.

- (ii) Carrier injection from the substrate may play a major role for the behaviour at the lower excitation energies. This is suggested since the resistance increase at photon energies below the STO bandgap can be explained by carrier compensation in analogy to the observations of Katsu *et al* [24] for $\text{La}_{1-x}\text{Sr}_x\text{MnO}_3/\text{SrTiO}_3$ heterostructures. There, injection of photogenerated electrons from the *n*-type-like STO into the film is discussed to compensate the hole doping of the manganite, which in turn leads to a resistance increase. We note that neither heating of the illuminated area nor parallel photoconduction in the SrTiO_3 substrate can cause the observed increase in resistance.

The different behaviour for photon energies around and above the STO bandgap is not in conflict with the above statement. For this case, carrier generation in the substrate is strongly enhanced due to excitation across the bandgap. Thus, the film might be flooded by electrons from the substrate, and one part of those photogenerated electrons may compensate the hole doping of the film, while the other part may act as free carriers in an induced electron-doped state of the film. However, the quasi-metallic conduction displayed in figure 1(b) appears quite different from the typical behaviour of metallic manganites, since the resistance peak is rather a distinct anomaly located between 100 and 110 K. At a similar temperature, a structural transition takes place in SrTiO_3 [29]. Thus, it seems to be possible that the photoconduction takes place in a (modified) interface-near region of the substrate, see also the next item.

- (iii) Photoconductivity data were taken on a bare as-purchased (untreated) reference substrate (figure 3(a)). This sample reaches a photoconductivity of more than three orders

of magnitude at 90 K already at visible excitation, which is decisively larger than the effect of the as-prepared LCMO/STO sample. Further, the resistance of the bare substrate is at least two orders of magnitude higher than that of the as-prepared LCMO/STO sample at all temperatures and at all excitation conditions used. This reference experiment conducted on a bare substrate indicates that the photoconduction of bare SrTiO_3 is not similar to the observation for the thin-film sample. However, the LCMO/STO interface may show modified properties, for instance due to an exchange of electrons or diffusion of oxygen.

- (iv) The intrinsic photoconductivity of the film itself, i.e. the photoinduced carrier generation in the film, for instance, by excitation across the polaron binding energy gap, appears to be rather small for this sample. No clear metal-insulator transition can be achieved under the conditions of illumination. Since the applied photon energies are large enough to overcome the typical polaron binding energy in manganites, the reason for this might be the above-discussed compensation of the hole carriers by electrons from the substrate.

The R - T characteristics of the *reduced* $\text{La}_{0.7}\text{Ca}_{0.3}\text{MnO}_3/\text{SrTiO}_3$ system is insulating in the dark, too (figure 2(a), thick black curve). However, there are decisive differences to the as-prepared case. The resistance values are several orders of magnitude higher. In contrast to the as-prepared case where the R - T dark characteristics is best fitted by the variable range hopping model, the data of the reduced system fits better to the activated polaron hopping or simple thermal activation models.

Illumination causes—in comparison to the as-prepared LCMO/STO sample—*pronounced* resistance changes. In the whole wavelength range used here (700–350 nm) photoexcitation induces an insulator-metal transition (IMT) and leads to large photoconductivity below the transition temperature.

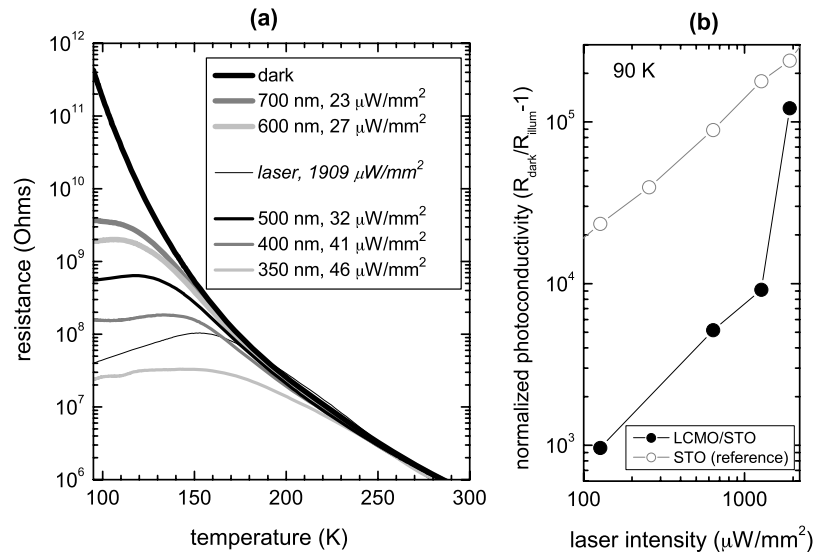


Figure 2. Reduced $\text{La}_{0.7}\text{Ca}_{0.3}\text{MnO}_3$ film on SrTiO_3 : (a) resistance measured as a function of temperature in the dark and under illumination with different photon energies. (b) Normalized photoconductivity (NPC) as calculated according to $\text{NPC} = \frac{R_{\text{dark}}}{R_{\text{illum}}} - 1$ of the reduced LCMO/STO sample at 90 K. Corresponding NPC values of the uncoated reduced STO reference sample (see also figure 3) are shown for comparison.

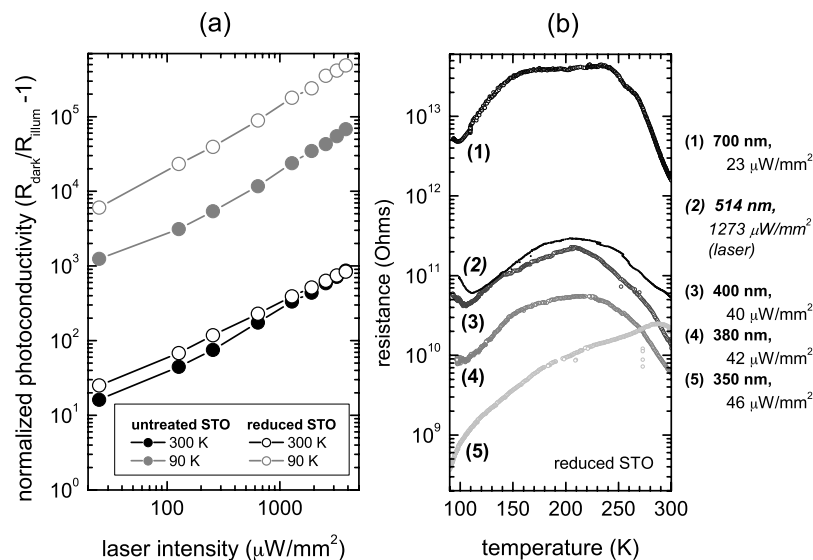


Figure 3. Photoresponse of uncoated SrTiO_3 crystals: (a) normalized photoconductivity (NPC) of an as-purchased (untreated) and a reduced STO sample at 300 and 90 K. (b) R - T -characteristics of the reduced STO reference sample under different illumination conditions. Note that curves (1) and (3)–(5) were acquired with (a comparatively small) constant photon flux, while curve (2) was measured under a much higher photon flux.

Although already infrared light (700 nm) generates a resistance drop of two orders of magnitude at 100 K, at constant photon flux the effect is enhanced with decreasing wavelength and reaches four orders of magnitude when the sample is excited with ultraviolet light (350 nm). Besides the wavelength, the intensity crucially influences the magnitude of the photoconductivity and the temperature of the IMT as has been tested by laser illumination with enlarged energy density (figure 2(b)). If the R - T -characteristics (figure 2(a)) at a fixed wavelength for the case of low intensity illumination (500 nm, $32 \mu\text{W mm}^{-2}$) and the case of high intensity

illumination (514 nm, $1909 \mu\text{W mm}^{-2}$) are compared, it can be stated that the phase transition becomes more distinct at high intensities. The temperature of the phase transition increases with increasing photon energy at constant photon flux and with increasing intensity at constant photon energy. The spectral dependence of the resistance (figure 4(b)) shows some slope changes in the sub-bandgap range. Most of them can be found also in the resistance spectrum of the bare reduced STO sample (figure 4(c)). In all resistance spectra, a steep resistance drop at the wavelength approximately corresponding to the STO bandgap is visible.

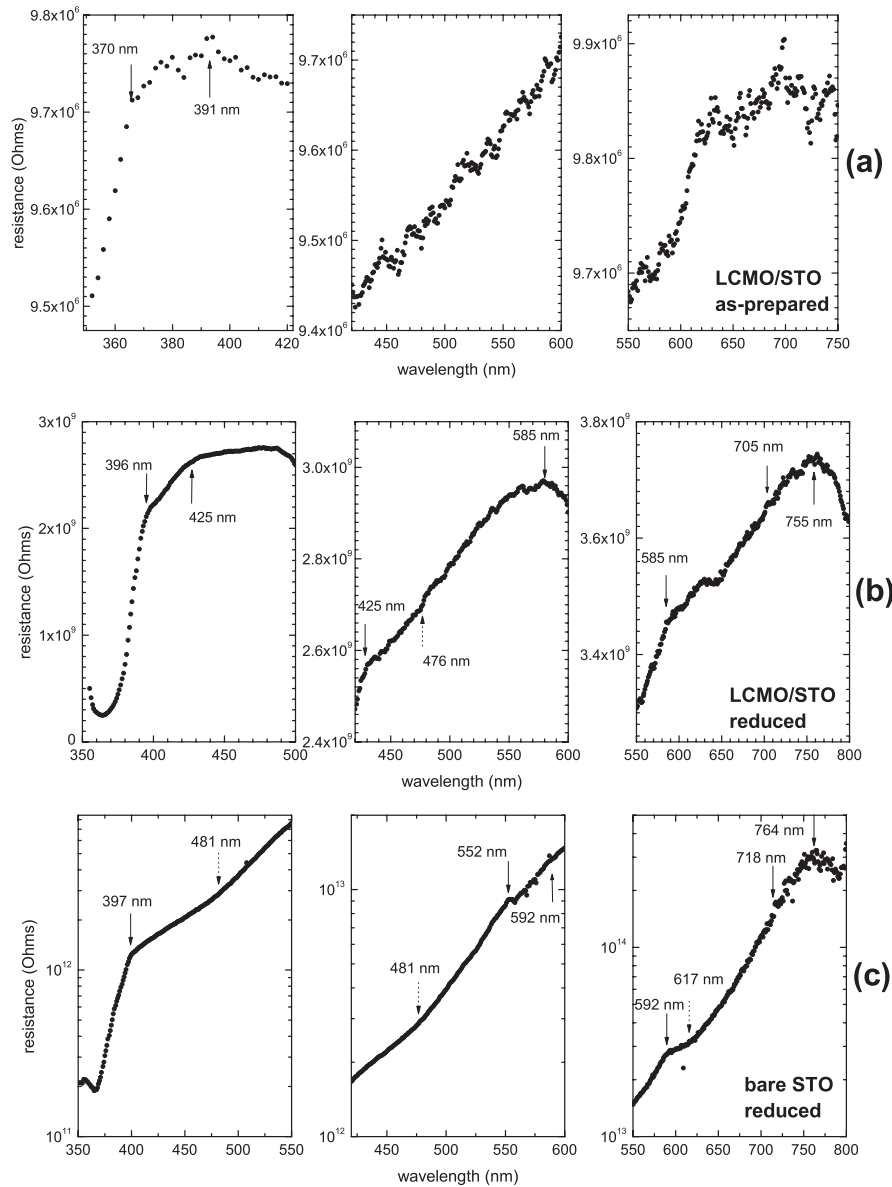


Figure 4. Resistance of (a) the as-prepared LCMO/STO heterostructure, (b) the reduced LCMO/STO heterostructure and (c) a bare reduced STO crystal as a function of illumination wavelength. The photon flux was kept constant during the data acquisition. Reproducible points of slope change, which can be attributed to electronic defect states, were extracted as described elsewhere [30] and are indicated by arrows. Note that, for reasons of readability of the spectra, the wavelength scales are partially different and that the resistance scale is logarithmic for part (c).

In the discussion of the mechanisms behind the large photoconductivity and the photoinduced IMT of the reduced sample we again have to consider the whole film–substrate system:

- (i) The similar sub-bandgap features in the resistance spectra of the bare STO (figure 4(c)) and the LCMO/STO heterostructure (figure 4(b)) and the steep resistance drop at the STO bandgap reveal an influence of the substrate at all wavelengths used here.
- (ii) According to our previous photoelectron spectroscopy study [26], the reduced LCMO film exhibits a manganese valence between +2 and +3 and is thus nominally electron-doped. Photogenerated electron injection from

the substrate would thus increase the carrier concentration in the film and lead to a resistance decrease, in agreement with the measurement.

- (iii) The question whether the measured photoconductivity is really based on carrier injection from the substrate or must be ascribed to parallel substrate conduction can be clarified from the data shown in figure 3(b). Here the R – T characteristics of a reduced reference STO sample is plotted for different illumination wavelengths. The curves show broad maxima at around 200 K; only the curve taken at 350 nm corresponds to metallic behaviour without any maximum. The positions of these maxima do not change with wavelength. Secondly, local minima which can be associated with the cubic-to-tetragonal phase transition

of STO, near 105 K, are visible. Those features do not appear in the corresponding LCMO/STO curves. Thus, we conclude that any parallel photoconduction in the substrate does not dominate. The fact that, as seen from the comparison of figures 4(a)–(c), the substrate resistance is much higher than the resistance of the film/substrate system also supports this statement.

Finally, we note that the photoresponse of the reduced LCMO/STO sample of the present study is quite similar as in our former observations on a reduced 10 nm thick $\text{La}_{0.7}\text{Ce}_{0.3}\text{MnO}_3$ film on STO [25], with regard to the weak photoresponse of the as-prepared system, the large photoconductivity of the reduced system and the significant influence of the substrate. This behaviour in turn is consistent with the similar Mn valences of the two systems [26] in both the as-prepared and the reduced state, despite the different nominal Mn valences.

4. Summary

The photoconduction of 10 nm thick $\text{La}_{0.7}\text{Ca}_{0.3}\text{MnO}_3$ films on SrTiO_3 was investigated within a comparative study of the as-prepared sample, an oxygen-reduced sample and bare untreated as well as oxygen-reduced SrTiO_3 substrates. Intensity- and wavelength-dependent resistance versus temperature characteristics as well as the spectral dependence of the resistance were measured. The reduced insulating LCMO/STO sample shows a pronounced photoconductivity: the resistance drops by five orders of magnitude at 100 K under visible 514 nm illumination, associated with a light-induced low-temperature metal state. The magnitude of the resistance change is comparable to the colossal magnetoresistance (CMR) effect. Photoexcitation has thus been shown to be highly effective in controlling the phase state of certain types of manganite films.

In contrast, the as-grown film sample, which is also insulating, shows smaller photoconduction, no clear light-induced metal–insulator transition and even a decrease of conductivity under illumination. We attribute this to the effect of carrier compensation by injection of electrons from the SrTiO_3 substrate. The substrate itself is photoconductive, but bare substrate data cannot explain the observed thin-film behaviour. Nevertheless, the photoconduction of the as-grown film sample shows an indication of parallel substrate photoconduction (reflecting the structural transition of SrTiO_3), which probably takes place at an interface-near region of SrTiO_3 .

Acknowledgment

This work was financially supported by the German Research Foundation (DFG, FOR 520).

References

- [1] Haghiri-Gosnet A-M and Renard J-P 2003 CMR manganites: physics, thin films and devices *J. Phys. D: Appl. Phys.* **36** R127–50
- [2] Gor'kov L P and Kresin V Z 2004 Mixed-valence manganites: fundamentals and main properties *Phys. Rep.* **400** 149–208
- [3] Dörr K 2006 Ferromagnetic manganites: spin-polarized conduction versus competing interactions *J. Phys. D: Appl. Phys.* **39** R125–50
- [4] Kiryukhin V, Casa D, Hill J P, Keimer B, Vigiliante A, Tomioka Y and Tokura Y 1997 An x-ray-induced insulator–metal transition in a magnetoresistive manganite *Nature* **386** 813–5
- [5] Miyano K, Tanaka T, Tomioka Y and Tokura Y 1997 Photoinduced insulator-to-metal transition in perovskite manganite *Phys. Rev. Lett.* **78** 4257–60
- [6] Hao J, He G, Lu D and Wong H-K 2000 Photoexcitation and transport characteristics in doped manganite thin films *Mater. Lett.* **46** 225–8
- [7] Gilibert A, Cauro R, Medici M G, Grenet J C, Wang H S, Hu Y F and Li Q 2000 Photoconductivity in manganites *J. Supercond.* **13** 285–90
- [8] Oshima H, Nakamura M and Miyano K 2001 Persistent photoconductivity in a ferromagnetic-metallic state of Cr-doped manganite thin film *Phys. Rev. B* **63** 075111
- [9] Moshnyaga V, Giske A, Samwer K, Mishina E, Tamura T, Nakabayashi S, Belenchuk A, Shapoval O and Kulyuk L 2004 Giant negative photoconductivity in $\text{La}_{0.7}\text{Ca}_{0.3}\text{MnO}_3$ thin films *J. Appl. Phys.* **95** 7360–2
- [10] Sheng Z G, Sun Y P, Dai J M, Zhu X B and Song W H 2006 Erasure of photoconductivity by magnetic field in oxygen-deficient $\text{La}_{2/3}\text{Sr}_{1/3}\text{MnO}_{3-\delta}$ thin films *Appl. Phys. Lett.* **89** 082503
- [11] Bah R, Bitok D, Rakhimov R R, Noginov M M, Pradhan A K and Noginova N 2006 Ferromagnetic resonance studies on colossal magnetoresistance films: effects of homogeneity and light illumination *J. Appl. Phys.* **99** 08Q312
- [12] Zhao K, Jin K-J, Huang Y-H, Lu H-B, He M, Chen Z-H, Zhou Y-L and Yang G-Z 2006 Laser-induced ultrafast photovoltaic effect in $\text{La}_{0.67}\text{Ca}_{0.33}\text{MnO}_3$ films at room temperature *Physica B* **373** 72–5
- [13] Kida N, Takahashi K and Tonouchi M 2007 Photoinduced phase transition in $\text{Pr}_{0.7}\text{Ca}_{0.3}\text{MnO}_3$ thin films probed via switching characteristics of terahertz radiation *Phys. Rev. B* **76** 184437
- [14] Matsubara M, Okimoto Y, Ogasawara T, Iwai S, Tomioka Y, Okamoto H and Tokura Y 2008 Photoinduced switching between charge and orbital ordered insulator and ferromagnetic metal in perovskite manganites *Phys. Rev. B* **77** 094410
- [15] Takubo N, Ogimoto Y, Nakamuro M, Tamaru H, Izumi M and Miyano K 2005 Persistent and reversible all-optical phase control in a manganite thin film *Phys. Rev. Lett.* **95** 017404
- [16] Fiebig M, Miyano K, Tomioka Y and Tokura Y 1998 Visualization of the local insulator–metal transition in $\text{Pr}_{0.7}\text{Ca}_{0.3}\text{MnO}_3$ *Science* **280** 1925–8
- [17] Fiebig M, Miyano K, Tomioka Y and Tokura Y 1999 Reflection spectroscopy on the photoinduced local metallic phase of $\text{Pr}_{0.7}\text{Ca}_{0.3}\text{MnO}_3$ *Appl. Phys. Lett.* **74** 2310–2
- [18] Sheng Z G, Sun Y P, Zhu X B, Dai J M, Song W H and Yang Z R 2007 Effect of bias current on the resistivity and photoconductivity of oxygen-deficient $\text{La}_{2/3}\text{Sr}_{1/3}\text{MnO}_{3-\delta}$ thin films *J. Appl. Phys.* **102** 093908
- [19] Chaudhuri S and Budhani R C 2008 Complementarity of perturbations driving insulator-to-metal transition in a charge-ordered manganite *Europhys. Lett.* **81** 17002
- [20] Westhäuser W, Schramm S, Hoffmann J and Jooss C 2006 Comparative study of magnetic and electric field induced insulator–metal transitions in $\text{Pr}_{1-x}\text{Ca}_x\text{MnO}_3$ films *Eur. Phys. J. B* **53** 323–31
- [21] Noginova N and Bonner C E 2005 Role of photoinduced heating in transient photoconductivity in CMR materials *Physica B* **363** 76–81

- [22] Jin K X, Chen C L and Zhao S G 2007 Photoinduced characteristics in $\text{La}_{0.67}\text{Ca}_{0.33}\text{MnO}_3$ film *J. Mater. Sci.* **42** 9617–21
- [23] Sagdeo P R, Choudhary R J and Phase D M 2010 Possible origin of photoconductivity in $\text{La}_{0.7}\text{Ca}_{0.3}\text{MnO}_3$ *J. Appl. Phys.* **107** 023709
- [24] Katsu H, Tanaka H and Kawai T 2001 Dependence of carrier doping level on the photo control of $(\text{La, Sr})\text{MnO}_3/\text{SrTiO}_3$ functional heterojunction *J. Appl. Phys.* **90** 4578–82
- [25] Beyreuther E, Thiessen A, Grafström S, Eng L M, Dekker M C and Dörr K 2009 Large photoconductivity and light-induced recovery of the insulator–metal transition in ultrathin $\text{La}_{0.7}\text{Ce}_{0.3}\text{MnO}_{3-\delta}$ films *Phys. Rev. B* **80** 075106
- [26] Beyreuther E, Grafström S, Eng L M, Thiele C and Dörr K 2006 XPS investigation of Mn valence in lanthanum manganite thin films under variation of oxygen content *Phys. Rev. B* **73** 155425
- [27] Holzapfel B, Roas B, Schultz L, Bauer P and Saemann-Ischenko G 1992 Off-axis laser deposition of $\text{YBa}_2\text{Cu}_3\text{O}_{7-\delta}$ thin films *Appl. Phys. Lett.* **61** 3178–80
- [28] Zandbergen H W, Freisem S, Nojima T and Aarts J 1999 Magnetoresistance and atomic structure of ultrathin films of $\text{La}_{0.73}\text{Ca}_{0.27}\text{MnO}_3$ on SrTiO_3 *Phys. Rev. B* **60** 10259–62
- [29] Rossella F, Galinetto P, Samoggia G, Trepakov V and Jastrabik L 2007 Photoconductivity and the structural phase transition in SrTiO_3 *Solid State Commun.* **141** 95–8
- [30] Beyreuther E, Grafström S, Eng L M, Thiele C and Dörr K 2006 Surface photovoltage spectroscopy for the investigation of Perovskite oxide interfaces *Mater. Res. Soc. Symp. Proc.* **902E** T7.5.1–11